The Effect of Solvation on the Mean Excitation Energy of Glycine

ARTICLE *in* JOURNAL OF PHYSICAL CHEMISTRY LETTERS · JANUARY 2010

Impact Factor: 7.46 · DOI: 10.1021/jz900100d

THE JOURNAL OF PHYSICAL CHEMISTRY Letters

pubs.acs.org/JPCL

The Effect of Solvation on the Mean Excitation Energy of Glycine

Kęstutis Aidas,[†] Jacob Kongsted,[‡] John R. Sabin,[‡,§] Jens Oddershede,[‡,§] Kurt V. Mikkelsen,[†] and Stephan P. A. Sauer*,[‡]

[†]Department of Chemistry, University of Copenhagen, Copenhagen, Denmark, [‡]Department of Physics and Chemistry, University of Southern Denmark, Odense, Denmark, and [§]Quantum Theory Project, Departments of Physics and Chemistry, University of Florida, Gainesville, Florida 32601

ABSTRACT Theoretical studies of energy deposition by fast ions on biological molecules are often carried out using isolated (gas phase) target molecules, while in fact the molecules are in an intracellular aqueous environment. The question then arises as to whether conclusions drawn from fast ion collisions with isolated biomolecules are applicable to the in vivo situation. In this contribution, we examine the prototypical case of the mean excitation energy of glycine for the isolated molecule and for the solvated molecule, using the polarizable quantum mechanics/molecular mechanics (QM/MM) approach employing both Hartree–Fock and density functional theory wave functions. The solvent shifts are approximately 2% of the isotropic mean excitation energy and are thus larger than the effect of electron correlation.

SECTION Biophysical Chemistry

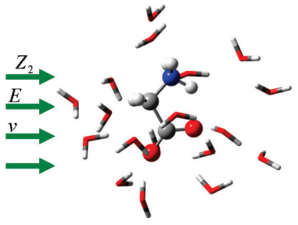

The major biological damage resulting from exposure of cells to radiation comes from either single (SSB) or double (DSB) strand breaks in DNA, and, to a lesser extent, from damage to intracellular proteins. Although a minority of damage is produced by direct hits of ions on either DNA or proteins, energy deposition by a fast ion in direct collision with a biomolecule, and the subsequent excitation and fragmentation of the target, must be understood. Massive particles, as opposed to photons, deposit energy in a molecule by collision with either the electrons (the dominant mechanism) or the nuclei of the molecule. The collision typically results in electronic excitation of the target molecule, followed by ionization, decay, emission of secondary radiation, or fragmentation. There are two situations to be considered. In the case of radiation damage, the fast ions typically pass through the biological sample doing damage as they pass through; a large ion velocity situation. For radiation therapy, it is desired to deposit the maximum amount of energy in the tumor. Ions deposit the most energy per unit path length at the Bragg peak, which occurs typically just before the ion comes to rest; a low velocity situation. This Letter is primarily concerned with the first case.

Energy transfer to a molecule by a fast ion is frequently described in terms of the energy loss per unit path length, or stopping power, of the target molecule.[1−3] [In the biologically related literature, the stopping power is often referred to as linear energy transfer, or LET, a misnomer, as there is nothing linear about it.] To avoid scatterer density differences, one frequently considers the stopping cross section $S(v)$:

$$-\frac{dE}{dx} = nS(v) \tag{1}$$

where n is the number density of the scatterers, and v is the projectile velocity. The cross section is further written in terms of the stopping number, $L(v)$ as

$$S(v) = \frac{4\pi e^4 {Z_1}^2 Z_2}{mv^2} L(v) \tag{2}$$

Here Z_1 and Z_2 are the projectile charge and target electron numbers, respectively. The simplest version of stopping theory, which we employ here, is valid for conditions where the projectile velocity is much larger than that of the target electrons, and leads to the Bethe/Born[1−6] form of the stopping number, which can be written

$$L(v) = \ln\frac{2mv^2}{I_0} - \frac{C(v)}{Z_2} + Z_1\frac{3\pi e^2 I_0}{2\hbar mv^3}\ln\frac{2mv^2}{I_0} - \frac{1.202{Z_1}^2}{v^2} \tag{3}$$

including the so-called Barkas and Bloch corrections,[1−6] which must be included if slow ion situations are to be considered. The first term on the right-hand side (rhs) of eq 3, the Bethe logarithm, is dominant at high projectile energies. If projectile velocities approaching the orbital electron velocities are considered, corrections to the Bethe logarithm must be made. The second term is referred to as the shell corrections, and is present to compensate for cases where the projectile velocity is not much greater than that of the target electrons, as are the last two terms. At large projectile velocity, $C(v)/Z_2$ consequently approaches zero.

Received Date: October 7, 2009
Accepted Date: November 10, 2009

DOI: 10.1021/jz900100d | *J. Phys. Chem. Lett.* **2010**, *1*, 242–245

The quantity I_0 is known as the mean excitation energy of the target, and is the target material constant for the problem. The mean excitation energy is defined as the first energy weighted moment of the dipole oscillator strength distribution (DOSD) of the target:

$$\ln I_0 = \frac{\sum_i f_{0i} \ln E_{0i}}{\sum_i f_{0i}} \quad (4)$$

Here $\{E_{0i}\}$ is the set of all electronic excitation energies for the target, and $\{f_{0i}\}$ is the set of the corresponding dipole oscillator strengths. When the dipole oscillator strength spectrum, df/dE, is fully known as a function of excitation energy, E, then I_0 may be evaluated from:[7]

$$\ln I_0 = \frac{\int \ln E \frac{df}{dE} dE}{\int \frac{df}{dE} dE} \quad (5)$$

The mean excitation energy measures the difficulty with which a target molecule can absorb energy from a massive projectile. Large mean excitation energies correspond to larger difficulty for the absorption of energy, and thus lead to lower stopping power.

For nonspherical molecules, one can also define an anisotropy in the mean excitation energy as[8]

$$A = Z_2 \ln \frac{I_0^y I_0^z}{(I_0^x)^2} \quad (6)$$

Previously[9,10] we have studied the mean excitation energy of glycine and compared it to that of alanine (unpublished results). In those cases, the DOSD was calculated, and the characteristics of the mean excitation energies of glycine and alanine were computed. However, in all cases, the calculations were carried out on the isolated amino acid molecule. As water is ubiquitous in the cell, it is certain that any biomolecule within the cell will be solvated. The question then arises if solvation will change the mean excitation properties of an amino acid. Answering that question is the purpose of this contribution, using glycine as the test case.

To model glycine in aqueous solution, we rely on the polarizable quantum mechanics/molecular mechanics (QM/MM) model,[11] which possesses the ability to model the effects of specific solute−solvent interactions in an effective and accurate manner. Especially explicit consideration of hydrogen bonding between the (polar) solvent water and the zwitterion plays a crucial role for an accurate description of the electronic structure for the solute. First a classical molecular dynamics (MD) simulation of 1 rigid glycine and 511 rigid water molecules was conducted to generate a number of molecular solute−solvent configurations to be used in the subsequent QM/MM calculations, where the QM region consists of the glycine molecule alone, and all water molecules are described by the same MM potential as in the MD simulation. We use either the Hartree−Fock (HF) or the density functional theory (DFT) description of the electronic structure of glycine. The basis set used is the same as in our previous vacuum studies of glycine and alanine.[9] In the DFT calculations, we employ the hybrid functional PBE0.[12,13] We compute the vertical excitation energies and oscillator strengths in the length gauge by the standard procedures of time-dependent HF/MM and DFT/MM theories as described in refs 11 and 14. In our previous studies[9,10] we could show that calculations on glycine in the gas phase with the same basis but in the velocity representation give essentially the same results. All excitation energies allowed by the finite basis set are calculated. As a result, we approximate the continuum with a finite number of discrete excitations (pseudostates) placed such that they represent the continuum. We have found that this discretization of the continuum works well when sums over the entire excitation spectrum are taken, but no significance attaches to the individual pseudostates. Finally, the mean excitation energy in solution is evaluated as a statistical average over the mean excitation energies of glycine in 120 molecular configurations extracted from the MD simulation.

Table 1. HF and DFT-Based *xx*, *yy*, and *zz* Components and Total Mean Excitation Energies (in eV) of Glycine in Vacuo and in Aqueous Solution

	HF		PBE0	
component	vacuo	water	vacuo	water
xx	69.12	67.75 ± 0.02	68.50	67.25 ± 0.02
yy	67.73	66.28 ± 0.01	67.27	65.56 ± 0.01
zz	76.77	75.69 ± 0.01	76.48	75.41 ± 0.01
total	71.10	69.79 ± 0.01	70.64	69.28 ± 0.01
anisotropy	3.39	3.56	3.68	3.56

In Table 1, we present the directional components, that is, the direction of the allowed polarization of the transition elements, and the total value of the mean excitation energy, I_0, for glycine in vacuo and in water obtained both at the HF and DFT/PBE0 levels of theory. The solvent shift is negative, which implies that the surrounding water molecules reduce the mean excitation energy of glycine and thus increase its stopping power. The effect of solvation is rather small. In both the HF and DFT calculations, it amounts to only 1.5% or 2% on average, which is significantly smaller than what is observed for the individual excitations.[15−18] For instance, n → π^* transitions normally exhibit a blue shift, when going from gas phase to water solution: acetone +4%, acrolein +7%, pyrazine +2%, pyrimidine +5%, and pyridazine +14%. For $\pi \rightarrow \pi^*$ transitions, one observes a red shift, for example, in acrolein of −8%. The solvent induced shifts on individual excitation energies are thus significantly larger than those on mean excitation energy, but can have opposite signs for different types of excitations. It is therefore not surprising that the solvent effect on the mean excitation energy is smaller.

Nevertheless, the solvent shift is still about three times larger than the effect of electron correlation, as exemplified here by the difference in the DFT/PBE0 and the HF results, which amount to less than 1%. This is in good agreement with previous DFT/B3LYP calculations on glycine and alanine, where the difference between HF and DFT calculations were found to be even smaller.[10]

In the case of oriented molecules, one can study the ratio of stopping of an incoming beam perpendicular or parallel to the molecular axis. This is related to the anisotropy defined in eq 6. Changes in the anisotropy due to the solvent or better

DOI: 10.1021/jz900100d | J. Phys. Chem. Lett. 2010, 1, 242–245

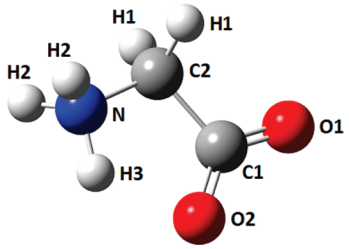

Figure 1. Structure and atom labeling of zwitterionic glycine.

treatment of electron correlation are thus sensitive probes for subtle differences in the behavior of the Cartesian components of the mean excitation energy. For glycine, we find that the changes in the ratio of the components of the mean excitation due to the solvent or electron correlation are small. However, we note that the small solvent shift has opposite signs at the HF and DFT level.

Summarizing, we can state that in the case of glycine gas-phase time-dependent HF calculations of the mean excitation energy can safely be used as an upper bound for the mean excitation energy and thus as a lower bound for the stopping power of glycine in solution, at least in the projectile velocity range where Bethe theory is appropriate. At lower projectile velocities, nearer to the Bragg peak, the mean excitation energy of the target system will no longer be the major factor determining projectile energy loss, and the effects of solvation might be considerable larger.

Finally, we list here the details of the QM/MM calculations and the MD simulation. For the QM/MM calculations, we have employed the polarizable QM/MM model[11] as implemented in the development version of the Dalton program.[19] The zwitterionic structure of glycine (in C_s symmetry, see Figure 1) was derived from a geometry optimization at the B3LYP[20]/aug-cc-pVTZ[21] level of theory combined with the polarizable continuum model[22] to account for the effects of bulk water. Partial point charges were derived from the CHelpG procedure,[23] which fits the atomic charges to reproduce the molecular electrostatic potential, using the B3LYP/aug-cc-pVTZ method in vacuum and constraints on the electric dipole moment. The Gaussian 03 program[24] was used for the geometry optimization and CHelpG calculation. To model solvent polarization, we assigned to the atomic sites of glycine isotropic dipole polarizabilities by partitioning the molecular polarizabilities computed at the B3LYP/aug-cc-pVTZ level using the LoProp approach[25] implemented in the Molcas program.[26] A 6−12-type Lennard-Jones (LJ) potential is used to model van der Waals interactions. The LJ parameters for glycine are listed in ref 27 and are due to the AMBER95 force field.[28] For the water molecules, we use the geometry taken from ref 29 and the polarizable potential of Ahlström et al.[30] The force field parameters for glycine and water molecules are collected in Table 2.

The MD simulation of 1 rigid glycine and 511 rigid water molecules was performed within the NVT ensemble at a temperature of 298.15 K using the Molsim program.[31] The cubic box length was set to 24.91 Å to reproduce the experimental density of liquid water. The velocity Verlet integration algorithm was employed with a time step of 2 fs along with use of periodic boundary conditions. The electrostatic and LJ interactions are truncated at half of the box length, and a reaction field correction is considered beyond this cutoff. The induced dipole moments were recalculated at every third time step with the relative tolerance of 10^{-7}. In addition, a linear damping scheme for the dipole−dipole interactions is employed as described in ref 32. The system was equilibrated for 200 ps, and the molecular configurations were recorded every 10 ps during the production run of 1.2 ns. In the QM/MM calculations, glycine is encapsulated in the QM region, and all water molecules are described by the Ahlström potential as in the MD simulation. We use a center of mass−center of mass based spherical cutoff distance of 12 Å for the water molecules. The inputs for the QM/MM calculations were made, and later statistical analysis of the results was performed using the Whirlpool program.[33]

Table 2. Force Field Parameters for Zwitterionic Glycine and Water Molecules[a]

molecule	atom	q	α	σ	ε
glycine	N	−0.373	0.8697	3.3400	0.1700
	O1	−0.571	1.0230	2.9600	0.2100
	O2	−0.597	0.8529	2.9600	0.2100
	C1	0.458	1.4817	3.3996	0.0860
	C2	−0.273	1.3779	3.3996	0.1700
	H1	0.158	0.3520	2.4714	0.0157
	H2	0.318	0.2928	1.0690	0.0157
	H3	0.323	0.2326	1.0690	0.0157
water	O	−0.6690	1.4400	3.1660	0.1555
	H	0.3345	0.0000	0.0000	0.0000

[a] Charges, q, are given in a.u., isotropic polarizabilities, α, are given in Å^3, and LJ parameters σ and ε are given in Å and kcal/mol, respectively.

AUTHOR INFORMATION

Corresponding Author:

*To whom correspondence should be addressed. E-mail: sauer@kiku.dk.

ACKNOWLEDGMENT This work was supported by grants from the Danish Center for Scientific Computing, the Carlsberg and Villum Kahn Rasmussen foundation, and the Danish Natural Science Research Council/The Danish Councils for Independent Research (J.K., K.V.M., and S.P.A.S.).

REFERENCES

(1) Bonderup, E. *Penetration of Charged Particles through Matter*, 2nd ed.; Fysik Instituts Trykkeri, Aarhus Universitet: Aarhus, Denmark, 1981.

(2) Ziegler, J. F.; Biersack, J. P.; Littmark, U. *The Stopping and Range of Ions in Solids*; Stopping and Ranges of Ions in Matter; Pergamon Press: Oxford, 1985; Vol. 1

(3) Janni, J. F. Energy Loss, Range, Path Length, Time-of-Flight, Straggling, Multiple Scattering, and Nuclear Interaction Probability: In Two Parts. Part 1. For 63 Compounds. Part 2. For Elements $1 \leq Z \leq 92$. *At. Data Nucl. Data Tables* **1982,** *27*, 147–339.

DOI: 10.1021/jz900100d | *J. Phys. Chem. Lett.* **2010,** *1*, 242–245

(4) Bethe, H. Zur Theorie des Durchgangs Schneller Korpuskularstrahlen Durch Materie. *Ann. Phys.* (*Leipzig*) **1930,** *397*, 325–400.
(5) Bethe, H. Bremsformel für Elektronen Relativistischer Geschwindigkeit. *Z. Phys.* **1932,** *76*, 293–299.
(6) Bethe, H. Molière's Theory of Multiple Scattering. *Phys. Rev.* **1953,** *89*, 1256–1266.
(7) Inokuti, M.; Karstens, W.; Shiles, E.; Smith, D. Y. Mean Excitation Energy for the Stopping Power of Silicon from Oscillator-Strength Spectra. Presented at the 2005 APS March Meeting, Los Angeles, Ca, March 21−25, 2005; http://meetings.aps.org/link/BAPS.2005.MAR.R1.55
(8) Sauer, S. P. A.; Sabin, J. R.; Oddershede, J. Calculated Molecular Mean Excitation Energies for Stopping and Straggling. *Nucl. Instrum. Methods B* **1995,** *100*, 458–463.
(9) Sauer, S. P. A.; Oddershede, J.; Sabin, J. R. Directional Dependence of the Mean Excitation Energy and Spectral Moments of the Dipole Oscillator Strength Distribution of Glycine and its Zwitterion. *J. Phys. Chem. A* **2006,** *110*, 8811–8817.
(10) Sabin, J. R.; Oddershede, J.; Sauer, S. P. A. Amino Acid Mean Excitation Energies and Directional Dependencies from Core and Bond Calculations. *AIP Proc.* **2008,** *CP1080*, 138–144.
(11) Kongsted, J.; Osted, A.; Mikkelsen, K. V.; Christiansen, O. The QM/MM Approach for Wavefunctions, Energies and Response Functions within Self-Consistent Field and Coupled Cluster Theories. *Mol. Phys.* **2002,** *100*, 1813–1828.
(12) Ernzerhof, M.; Scuseria, G. E. Assessment of the Perdew−Burke−Ernzerhof Exchange-Correlation Functional. *J. Chem. Phys.* **1999,** *110*, 5029–5036.
(13) Adamo, C.; Barone, V. Toward Reliable Density Functional Methods without Adjustable Parameters: The PBE0 Model. *J. Chem. Phys.* **1999,** *110*, 6158–6170.
(14) Nielsen, C. B.; Christiansen, O.; Mikkelsen, K. V.; Kongsted, J. Density Functional Self-Consistent Quantum Mechanics/Molecular Mechanics Theory for Linear and Nonlinear Molecular Properties: Applications to Solvated Water and Formaldehyde. *J. Chem. Phys.* **2007,** *126*, 154112.
(15) Kongsted, J.; Osted, A.; Mikkelsen, K. V.; Åstrand, P.-O.; Christiansen, O. Solvent Effects on the n → π^* Electronic Transition in Formaldehyde: A Combined Coupled Cluster/Molecular Dynamics Study. *J. Chem. Phys.* **2004,** *121*, 8435–8445.
(16) Aidas, K.; Kongsted, J.; Osted, A.; Mikkelsen, K. V.; Christiansen, O. J. Coupled Cluster Calculation of the n → π^* Electronic Transition of Acetone in Aqueous Solution. *J. Phys. Chem. A* **2005,** *109*, 8001–8010.
(17) Kongsted, J.; Mennucci, B. How to Model Solvent Effects on Molecular Properties Using Quantum Chemistry? Insights from Polarizable Discrete or Continuum Solvation Models. *J. Phys. Chem. A* **2007,** *111*, 9890–9900.
(18) Aidas, K.; Møgelhøj, A.; Nilsson, E. J. K.; Johnson, M. S.; Mikkelsen, K. V.; Christiansen, O.; Söderhjelm, P.; Kongsted, J. On the Performance of Quantum Chemical Methods to Predict Solvatochromic Effects: The Case of Acrolein in Aqueous Solution. *J. Chem. Phys.* **2008,** *128*, 194503.
(19) *Dalton: a molecular electronic structure program*, release 2.0, 2005. See http://www.kjemi.uio.no/software/dalton/dalton.html.
(20) Becke, A. D. Density-Functional Thermochemistry. III. The Role of Exact Exchange. *J. Chem. Phys.* **1993,** *98*, 5648–5652.
(21) Kendall, R. A.; Dunning, T. H.; Harrison, R. J. Electron Affinities of the First-Row Atoms Revisited. Systematic Basis Sets and Wave Functions. *J. Chem. Phys.* **1992,** *96*, 6796–6806.
(22) Tomasi, J.; Mennucci, B.; Cammi, R. Quantum Mechanical Continuum Solvation Models. *Chem. Rev.* **2005,** *105*, 2999–3094.
(23) Breneman, C. M.; Wiberg, K. B. Determining Atom-Centered Monopoles from Molecular Electrostatic Potentials. The Need for High Sampling Density in Formamide Conformational Analysis. *J. Comput. Chem.* **1990,** *11*, 361–373.
(24) Frisch, M. J.; Trucks, G. W.; Schlegel, H. B.; Scuseria, G. E.; Robb, M. A.; Cheeseman, J. R.; Montgomery, J. A., Jr.; Vreven, T.; Kudin, K. N.; Burant, J. C.; Millam, J. M.; Iyengar, S. S.; Tomasi, J.; Barone, V.; Mennucci, B.; Cossi, M.; Scalmani, G.; Rega, N.; Petersson, G. A.; Nakatsuji, H.; Hada, M.; Ehara, M.; Toyota, K.; Fukuda, R.; Hasegawa, J.; Ishida, M.; Nakajima, T.; Honda, Y.; Kitao, O.; Nakai, H.; Klene, M.; Li, X.; Knox, J. E.; Hratchian, H. P.; Cross, J. B.; Bakken, V.; Adamo, C.; Jaramillo, J.; Gomperts, R.; Stratmann, R. E.; Yazyev, O.; Austin, A. J.; Cammi, R.; Pomelli, C.; Ochterski, J. W.; Ayala, P. Y.; Morokuma, K.; Voth, G. A.; Salvador, P.; Dannenberg, J. J.; Zakrzewski, V. G.; Dapprich, S.; Daniels, A. D.; Strain, M. C.; Farkas, O.; Malick, D. K.; Rabuck, A. D.; Raghavachari, K.; Foresman, J. B.; Ortiz, J. V.; Cui, Q.; Baboul, A. G.; Clifford, S.; Cioslowski, J.; Stefanov, B. B.; Liu, G.; Liashenko, A.; Piskorz, P.; Komaromi, I.; Martin, R. L.; Fox, D. J.; Keith, T.; Al-Laham, M. A.; Peng, C. Y.; Nanayakkara, A.; Challacombe, M.; Gill, P. M. W.; Johnson, B.; Chen, W.; Wong, M. W.; Gonzalez, C.; Pople, J. A. *Gaussian 03*, revision C.02; Gaussian, Inc.: Wallingford, CT, 2004.
(25) Gagliardi, L.; Lindh, R.; Karlström, G. Local Properties of Quantum Chemical Systems: The LoProp Approach. *J. Chem. Phys.* **2004,** *121*, 4494–4500.
(26) Karlström, G.; Lindh, R.; Malmqvist, P.-Å.; Roos, B. O.; Ryde, U.; Veryazov, V.; Widmark, P.-O.; Cossi, M.; Schimmelpfennig, B.; Neograd, P.; Seijo, L. MOLCAS: A Program Package for Computational Chemistry. *Comput. Mater. Sci.* **2003,** *28*, 222–239.
(27) Takahashi, H.; Kawashima, Y.; Nitta, T.; Matubayasi, N. A Novel Quantum Mechanical/Molecular Mechanical Approach to the Free Energy Calculation for Isomerization of Glycine in Aqueous Solution. *J. Chem. Phys.* **2005,** *123*, 124504.
(28) Cornell, W. D.; Cieplak, P.; Bayly, C. I.; Gould, I. R.; Merz, K. M.; Ferguson, D. M.; Spellmeyer, D. C.; Fox, T.; Caldwell, J. W.; Kollman, P. A. A Second Generation Force Field for the Simulation of Proteins, Nucleic Acids, and Organic Molecules. *J. Am. Chem. Soc.* **1995,** *117*, 5179–5197.
(29) Billing, G. D.; Mikkelsen, K. V. Dynamical Model for S_N2 Reactions in Solution. The $Cl^- + CH_3Cl \rightarrow ClCH_3 + Cl^-$ Reaction. *Chem. Phys.* **1994,** *182*, 249–262.
(30) Ahlström, P.; Wallqvist, A.; Engström, S.; Jönsson, B. A Molecular Dynamics Study of Polarizable Water. *Mol. Phys.* **1989,** *68*, 563–581.
(31) Linse, P. MOLSIM is an integrated MD/MC/BD simulation program belonging to the MOLSIM package, version 3.3.0, December 05, 2001.
(32) van Duijnen, P. T.; Swart, M. Molecular and Atomic Polarizabilities: Thole's Model Revisited. *J. Phys. Chem. A* **1998,** *102*, 2399–2407.
(33) Aidas, K. Whirlpool: A QM/MM analysis program; Copenhagen University, 2009. For more information contact: kestas@theory.ki.ku.dk.

DOI: 10.1021/jz900100d | *J. Phys. Chem. Lett.* **2010,** *1*, 242–245